

**Effect of the AMD-3100
on survival of expanded
ischemic flap**

Hii Sun Jeong

Department of Medicine

The Graduate School, Yonsei University

**Effect of the AMD-3100
on survival of expanded
ischemic flap**

Directed by Professor Kwan Chul Tark

Doctoral Dissertation
submitted to the Department of Medicine,
the Graduate School of Yonsei University
in partial fulfillment of the requirements
for the degree of Doctor of Philosophy

Hii Sun Jeong

December 2013

This certifies that the Doctoral
Dissertation of
Hii Sun Jeong is approved.

Thesis Supervisor: Kwan Chul Tark

Thesis Committee Member#1: Dae Hyun Lew

Thesis Committee Member#2: Hye Kyung Lee

Thesis Committee Member#3: Yoon Woo Koh

Thesis Committee Member#4: Chul Hoon Kim

The Graduate School
Yonsei University

December 2013

ACKNOWLEDGEMENTS

Undertaking this doctoral degree has been a truly life-changing experience for me, and it would not have been possible without the support and guidance that I received from many people.

I would like to express my special appreciation and thanks to my supervisor Professor Kwan-Chul Tark. This work would not have been possible without his guidance, support and encouragement.

I would also like to thank Professors Dae-Hyun Lew, Yoon-Woo Koh, and Chul-Hoon Kim for their valuable advice, constructive criticism and extensive discussion regarding to my work.

I am as well extremely indebted to Prof. Hye-Kyung Lee for her constant support, encouragement and her special mentions.

My special thanks go to a veterinarian, Jooyeon Suk for her generous support, and to my friends, Yuri Kim and Sejung Park for their warm and unfailing encouragement.

Last but not least, I would like to pay high regards to my father, Jong-Hwa Jeong, my mother Jung-Ho Seo, my nephew John, my niece Clara, and my sister Hee-Jin for their sincere encouragement.

Hii-Sun Jeong..

<TABLE OF CONTENTS>

ABSTRACT	1
I. INTRODUCTION	3
II. MATERIALS AND METHODS	7
1. Animals	7
2. Classification of experimental and control groups by administration of AMD-3100	7
(A) Preliminary study about determination of optimal dosage and route of administration for AMD-3100	7
(B) Preliminary study on the effect of AMD-3100 and inserting silicone sheets to block the neovascularization from the bed of a classical unexpanded flap	8
(C) Main study on the effects of treatment with AMD-3100 in the expanded flap model	8
3. Injection protocol for AMD-3100(EPC modulator, Mozobil [®])	9
4. Expanded skin flap animal model	9
5. Differentiation and mobilization of EPCs from bone marrow hematopoietic stem cells following injection of AMD-3100	12
(A) Bone marrow harvest	12
(B) Gelatin zymography of active MMP-9	12
(C) Flow cytometry analysis of peripheral blood cells	13
6. Measurement of survival area of flaps and blood flow	13
(A) Evaluation of survival area of flaps	13
(B) Physiologic assessment of blood flow by laser Doppler	14
7. Histology	14
(A) Quantitative measurement of vascularization	14
(B) Measurement of expressions of VEGF, SDF-1, and HIF-1 α	

in tissue	15
8. Western blot analysis	15
9. Quantitative real-time reverse transcriptase polymerase chain reaction(RT-PCR)	16
10. Statistical analysis	18
III. RESULTS	19
1. Selection of the optimal dosage and injection route of AMD-3100	19
2. Differentiation and mobilization of EPC from bone marrow hematopoietic stem cells following injection of AMD-3100	21
(A) Gelatin zymography of active MMP-9	21
(B) Flow cytometry of peripheral blood cells	22
3. The survival area of flaps	24
(A) Preliminary study of survival rate in unexpanded flaps	24
(B) Main study of survival rate in expanded flaps	27
4. Physiologic assessment of blood flow by laser Doppler	30
5. Histology	30
(A) Quantitative measurement of vascularization	30
(B) Density of VEGF, SDF-1 and HIF-1 α in tissue flaps	33
6. Western blot analysis	37
7. Real time quantitative RT-PCR of VEGFA, VEGFR2, NOS3, SDF-1, and HIF-1 α	39
IV. DISCUSSION	40
V. CONCLUSION	47
REFERENCES	50
ABSTRACT (IN KOREAN)	56

LIST OF FIGURES

Figure 1. Design of expanded ischemic random pattern skin flap	11
Figure 2. Design and operation	11
Figure 3. Survival rate of flap according to dosage of AMD-3100	20
Figure 4. MMP-9 zymography	21
Figure 5. Fraction patterns of CD34/VEGFR2 cells	22
Figure 6. Fraction pattern of VEGFR2 cells in peripheral blood	23
Figure 7. Fraction pattern of double VEGFR2+/CD34+ cells in peripheral blood	23
Figure 8. Photographs depicting flap survival in the preliminary study of unexpanded flaps	25
Figure 9. Survival rates of flaps in the preliminary Study of unexpanded flaps	26
Figure 10. Photographs depicting flap survival in the main study	28
Figure 11. Survival rate of flaps in the main study	29
Figure 12. Vessel areas and counts by immunohistochemical staining for CD31	32
Figure 13. Immunohistochemical staining for CD31	33

Figure 14. Density of VEGF in flap tissue	34
Figure 15. Immunohistochemical staining for VEGF	35
Figure 16. Immunohistochemical staining for SDF-1	36
Figure 17. Immunohistochemical staining for HIF-1 α	36
Figure 18. Western blot analysis of VEGF	37
Figure 19. Western blot analysis of SDF-1	38
Figure 20. Western blot analysis of HIF-1 α	38
Figure 21. Real time quantitative RT-PCR of VEGF, VEGFR2, NOS3, SDF-1, and HIF-1 α	39

LIST OF TABLES

Table 1. Classification of groups of rats in the preliminary study	8
Table 2. Classification of main study group	9
Table 3. Survival rate of flaps(%) according to the concentrations of AMD-3100	19
Table 4. Survival rate of flaps according to injection routes of AMD-3100	20
Table 5. The survival rate of flaps in the preliminary study of unexpanded flaps	25
Table 6. The survival rate of flaps in the main study	28
Table 7. Blood flow measured by laser Doppler	30
Table 8. Vessel area and vessel number	31
Table 9. Density of VEGF	34

ABSTRACT

Effect of the AMD-3100 on survival of expanded ischemic flap

Hii Sun Jeong

*Department of Medicine
The Graduate School, Yonsei University*

(Directed by Professor Kwan Chul Tark)

Vascular endothelial growth factor (VEGF) increased in expanded flap promotes vascularization, increasing the survival rate of expanded ischemic skin flaps. AMD-3100 is a recently developed inhibitor of chemokine receptor 4 (CXCR4), which inhibits binding between CXCR4 on hematopoietic stem cells and stromal cell-derived factor-1 (SDF-1) in the bone marrow. AMD-3100 contributes to vasculogenesis, which provides EPCs to the ischemic area of the flaps. The purpose of this study is to devise an expanded ischemic flap model, and to investigate the role of AMD-3100 in expanded ischemic flaps by confirming its effect on mobilization of stem cells from the bone marrow.

Male Sprague-Dawley rats were used as an animal research model for expanded ischemic skin flaps. First, in a preliminary study, we determined the optimal injection route and dosage of AMD-3100 and investigated the effect of AMD-3100 and silicone sheet insertion between the flap and recipient area. For the main experiments, the rats were divided four groups (n=10 rats per group), including: (1) untreated and not expanded (group I), (2) untreated and expanded (group II), (3) treated with AMD-3100 and not expanded (group III), and (4) treated with AMD-3100 and expanded (group IV). To determine the effects of injection of AMD-3100 on the differentiation and mobilization of hematopoietic stem cells to EPCs, we used flow cytometry using surface markers CD34, VEGFR2, and CD133 and gelatin zymography techniques for active matrix metalloproteinase-9 (MMP-9) in the bone marrow. Flap survival and neovascularization were assessed using photometrics, histology (CD31, VEGF, SDF-1, HIF-1 α), laser Doppler analysis, western blotting (VEGF, SDF-1, HIF-1 α), and real time quantitative RT-PCR (VEGFA, SDF-1, HIF-1 α , NOS3, and VEGFR2).

The level of active MMP-9 in the bone marrow was significantly higher in the AMD-3100-treated rats (groups III and IV) than in untreated rats (groups I and II) ($p<0.05$). The fraction of EPCs (VEGFR2+CD34+, double-positive) in the peripheral blood was significantly greater rats treated with AMD-3100 with expanded skin flaps (group IV) than in any other group at postoperative days 1 and 2 ($p<0.05$). At the same days, the fraction of single-positive VEGFR2+ cells in the peripheral blood of AMD-3100-treated rats without expanded flaps (group III) was significantly greater than in any other group ($p<0.05$). The expression of VEGF by immunohistochemistry was significantly increased in groups II, III, and IV in comparison with group I ($p<0.05$). The expression levels of SDF-1 and VEGFR2 were increased only in group III ($p<0.05$). The expression levels of NOS3 and hypoxia-inducible factor 1 α (HIF-1 α) were not increased following AMD-3100 injection and tissue expansion (group IV, $p>0.05$). Treatment with AMD-3100(group III and IV) increased both the number and area of blood vessels ($p<0.05$).

When compared with rats in group I, there were no statistically significant differences in the survival area or physiologic microcirculation in rats from the other groups ($p>0.05$). However, in the preliminary study, injection of AMD-3100 significantly increased the survival area of conventional flaps compared with control rats that had received injection of PBS ($p<0.05$). However, the survival area was decreased by insertion of a silicone layer between the flap and recipient site ($p<0.05$).

Treatment with AMD-3100 increased the mobilization of bone marrow-derived EPCs to the peripheral blood at the flap, regardless of tissue expansion. This endogenous neovascularization induced by AMD-3100 may be a result of the increase in both the area and number of vessels, as well as paracrine augmentation of the expression of VEGF and EPCs. However, the presence of a tissue expander at the flap could block the neovascularization between the flap and the recipient, and did not affect the survival area or physiologic blood flow in the microcirculation of the flap regardless of AMD-3100 treatment and expansion.

Key words: endothelial progenitor cell, hematopoietic stem cell, tissue expansion, ischemic flap, AMD-3100, CXCR4 inhibitor, plerixafor

Effect of AMD-3100 on survival of expanded ischemic flap

Hii Sun Jeong

Department of Medicine

The Graduate School, Yonsei University

(Directed by Professor Kwan Chul Tark)

I. INTRODUCTION

The use of a skin flap to cover soft tissue defects makes wound healed by primary repair and minimizes the incidence of wound contraction and scar formation. The use of skin flaps is one of the best reconstruction methodologies to preserve function such as flexibility of joints. However, the skin flap method may be limited in that the angiosome varies according to the character of the flap and the choice of optimal flap is sometimes limited depending upon the nature of the defect. Tissue expansion of the skin and soft tissue adjacent to the defect as an additional reconstructive modality provides advantages such as identical skin color, texture and skin appendage to that of the defect.

Advancing the expanded portion of the tissue to cover the defect of the recipient in the expanded flap reduces donor site morbidity and provides good cosmetic results. In cases of scanty donor tissue or the possibility of growth of

children (such as separation of conjoined twins or removal of congenital giant nevus) tissue expansion is necessary and appropriate.^{1,2}

There are several studies supporting the use of tissue expansion reported in the literature. Neuman, who first reported the method of tissue expansion, inserted a balloon beneath the skin to expand the tissue by continuous mechanical stretching and successfully reconstructed the external ear.³ Radovan used a silicone balloon to expand the skin and soft tissue for breast reconstruction,⁴ and Austad utilized a self-inflatable tissue expander.⁵ Codivilla applied the tissue expansion method to bones, and Illizarov and McCarthy employed this technique to distraction of the ilium and mandible.⁶⁻⁸ Currently, distraction osteogenesis is regarded as the most appropriate reconstruction method for bone gaps in pediatric patients for whom it is necessary to consider their natural growth during regeneration of the bone and soft tissue. Vacuum assisted closure, which promotes proliferation of fibroblasts through progressive mechanical stretching, is based on a similar concept.⁹

The region under tissue expansion has a favorable microenvironment for tissue regeneration. Platelet-derived growth factor (PDGF) and epidermal growth factor (EGF) accumulate in the proximity of the tissue expander and promote epithelial cell development via strain. Additionally transforming growth factor- β (TGF- β) promotes the formation of extracellular matrix. Tissue expansion takes place due to increased cell proliferation following activation of protein kinase leading to intracellular signal transduction.¹⁰

The length of viable area of the expanded flap that can survive under relatively low partial pressure of oxygen is increased by as much as 117% compared with that of the surgical delay procedure.^{11,12} Consequently, VEGF expression is significantly greater around the tissue expander, as compared with the original flap, as a result of continued VEGF expression under the conditions of constant low partial pressure of oxygen.^{13, 14}

Expression of growth factors such as VEGF, PDGF and EGF is increased in environments that require tissue regeneration. Stem cells migrate from the bone marrow to the peripheral blood, differentiate into endothelial progenitor cells (EPCs), and proliferate as EPCs. The microenvironment that produces growth factors such as VEGF, PDGF, and EGF can be likened to soil, and the EPCs can be likened to seeds planted in this soil.¹⁵ In order to improve the survival rate of the expanded flap, there should be an increase in angiogenesis and vasculogenesis, which requires a favorable microenvironment with over-expression of VEGF and mobilization of greater numbers of precursor cells such as EPCs. It has been shown that, following injury to a blood vessel, bone marrow-derived EPCs proliferate, differentiate and subsequently move to the peripheral blood where they participate in vasculogenesis.¹⁵ It has also been shown that transplant of cultured vascular EPCs leads to the localization and proliferation of these cells at the ischemic regions of skin flaps, as well as increased survival rates of the flaps.^{16, 17}

C-X-C chemokine receptor type 4 (CXCR4) is a cell surface receptor on bone

marrow hematopoietic stem cells. CXCR4 binds to stromal cell-derived factor 1 (SDF-1) in the bone marrow, promoting homing of hematopoietic stem cells to the bone marrow.¹⁸ AMD-3100, a recently developed iCXCR4 inhibitor, which is injected subcutaneously. When AMD-3100 is pre-treated with VEGF, these inhibits binding between CXCR4 on hematopoietic stem cells and SDF-1 in the bone marrow. By facilitating mobilization and differentiation of hematopoietic stem cells, the number of EPCs and mesenchymal cells in the peripheral blood rises by one hundredfold.¹⁸ In fact, AMD-3100 is now clinically used with pretreated granulocyte colony-stimulating factor (G-CSF) to promote mobilization of hematopoietic stem cells to the peripheral blood in patients with non-Hodgkin's lymphoma or multiple myeloma who require stem cell autotransplantation.^{19,20}

If treatment with AMD-3100 increases mobilization of EPCs in expanded flap tissues, it is possible that a smaller harvested donor flap could reconstruct a larger defect after expansion and therefore reduce donor site morbidity. It may also make it possible to reduce patient discomfort by reducing expansion time. Finally, the survival of expanded flaps may be improved by treatment with AMD-3100 by promoting vasculogenesis through expression of VEGF and mobilization of EPCs.

The purpose of this study is to devise an expanded ischemic flap model and to investigate the role of AMD-3100 in expanded ischemic flaps by demonstrating its effect on mobilization of EPCs from the bone marrow.

II. MATERIALS AND METHODS

1. Animals

The study utilized male Sprague-Dawley rats (body weight, 300 ~ 400g). All animal procedures were carried out according to a protocol approved by the Yonsei University Animal Care Committee. Isoflurane (Aerane[®], Ilsung Pharmaceuticals, Seoul, Korea) was used as an inhalation anesthetic. Zolazepam-tiletamine mixture (30mg/kg, Zoletil[®], Virbac, Carrs, France) and xylazine (10mg/kg, Rumpun[®], Bayer, Seoul, Korea) were administered as needed, by intraperitoneal injection.

2. Classification of experimental and control groups by administration of AMD-3100 and procedure

(A) Preliminary study for determination of optimal dosage and route of administration for AMD-3100

Classical dorsal axial patterned flaps (3cm x 9cm) were prepared on the backs of 42 rats without insertion of silicone. After preparation of skin flaps, groups of rats were divided by dosage of AMD-3100 (5mg/kg or 10mg/kg) and injection route (subcutaneous, intravenous or intraperitoneal) (n=7 rats per group). Following injection of AMD-3100, vasculogenesis and angiogenesis were measured by the survival area and photographically analyzed using Image J[®] software (NIH-Scion Corporation, Bethesda, MD, USA).

(B) Preliminary study on the effects of AMD-3100 and insertion of silicone sheets to block neovascularization from the bed of a classical unexpanded flap.

A total of 28 rats were divided into four groups (n=7 rats per group). Classical caudal based axial patterned dorsal skin flaps (3cm x 9cm) were elevated for all rats. A silicone sheet were placed between the elevated flap and the bed in groups B and D, but not in groups A and C. AMD-3100 was injected into rats in groups C and D in accordance with the optimal dosage and route determined above (Table 1). AMD-3100 was not administered to rats in groups A and B, and instead an equivalent amount of phosphate-buffered saline (PBS) was administered.

Table 1. Classification of groups of rats in the preliminary study

Group	Group A	Group B	Group C	Group D
AMD-3100	- (PBS)	- (PBS)	+	+
Silicone sheet	-	+	-	+

PBS: Phosphate buffered solution

(C) Main study on the effects of treatment with AMD-3100 in the expanded flap model

A total of 40 rats were divided into four groups (n= 10 rats per group) as listed in Table 2: Group I (control group, skin random pattern flap [3cm x 9cm],

elevation without AMD-3100 injection), Group II (flap expansion, without AMD-3100 injection), Group III (flap elevation and treatment with AMD-3100 injection), and Group IV (flap expansion and treatment with AMD-3100 injection). Rats that did not receive AMD-3100 were injected with an equivalent volume of PBS.

Table 2. Classification of main study group

Group	Group I (control)	Group II	Group III	Group IV
AMD-3100	- (PBS)	- (PBS)	+	+
Expansion	-	+	-	+

PBS: Phosphate buffered solution

3. Injection protocol for AMD-3100 (EPC modulator, Mozobil®)

Thirty minutes, 24 hours, and 48 hours after flap elevation, the 10mg/kg of AMD-3100 (Sigma, St Louis, MO, USA) was injected subcutaneously at the mid-point between the scapulae, 2 cm away from the distal portion of the flap. This dosage and route of administration were determined to be optimal in the preliminary experiments.

4. Expanded skin flap animal model

The design for tissue expansion of ischemic skin flaps is as shown in Figure 1.

A flap based on the tail measuring 3.0×9.0 cm was elevated on the back of each rat, as shown in Figure 2. The proximal portion of the flap was created at the ischial protuberance, and a 1.0 cm area from the distal edge of the flap was removed for replacement by the expanded skin flap. The flap consisted of 3 layers (skin, panniculus carnosus, and submuscular connective tissue), and did not include axial vessels. The edge of expanded skin flap was repaired with #4-0 nylon continuous suture technique by including bed and donor site to maintain the expansion and prevent vessel embedding between the flap and recipient site. In order to block blood flow from the floor, a silicone sheet (0.13 mm thick, 4cm x 11cm, Bioplexus Corporation[®], CA, USA) was placed under the flap and routine dressing was not enforced.

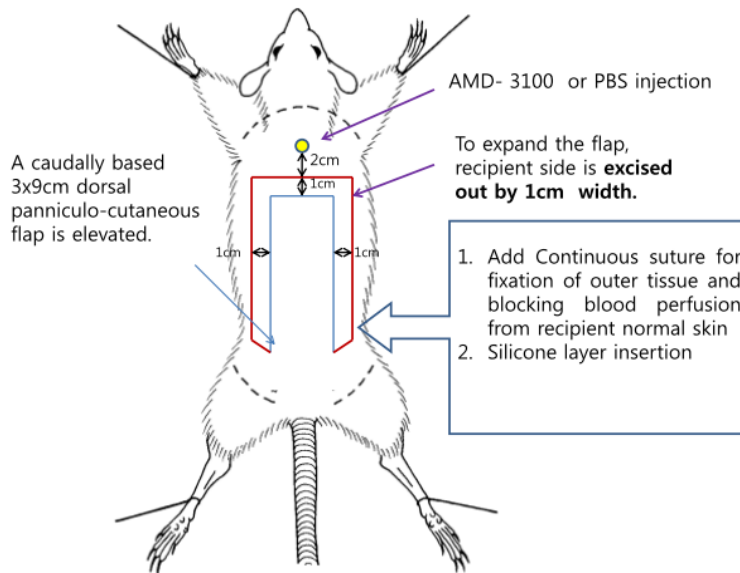


Figure 1. Design of expanded ischemic random pattern skin flap

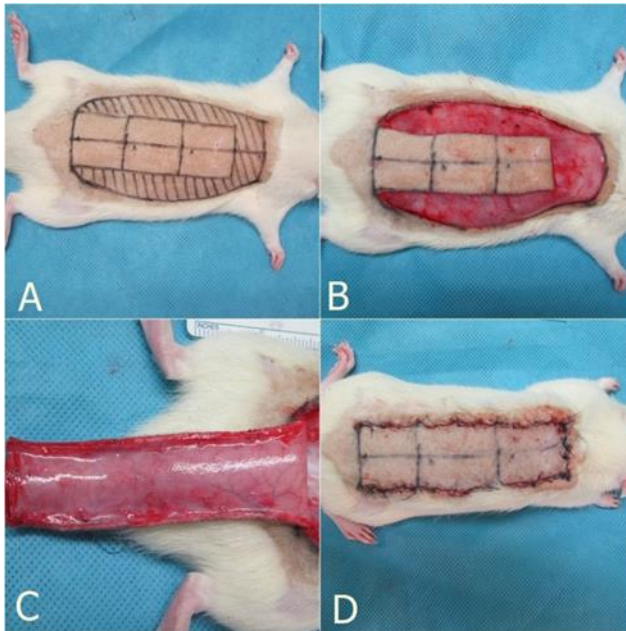


Figure 2. Design and operation (A) Flap elevation; (B) Edge of the distal flap removed for skin expansion; (C) Flap elevation above the submuscular connective tissue; (D) Silicone placement on the floor and final suture state.

5. Differentiation and mobilization of EPCs from bone marrow hematopoietic stem cells following injection of AMD-3100

After collection of whole blood at 24 hours and 48 hours postoperatively, we harvested bone marrow from the femurs of four rats from each group.

(A) Bone marrow harvest

After shaving and sterilization with alcohol and povidone, both right and left femurs and tibias were obtained from rats at postoperative day 2. Bone marrow was harvested from both articular areas by washing with sterile PBS using a 5 ml syringe. The collected solution was centrifuged (150xg, 10 min), and the supernatant was immediately stored at -70°C.

(B) Gelatin zymography for active MMP-9

The concentration of protein in each bone marrow sample was quantified using the Bradford Method protein assay kit (Bio-Rad Laboratories, Hercules, CA, USA), which is based on a bovine gamma globulin standard.

Each sample was separated by electrophoresis on 10% polyacrylamide gel containing 0.1% gelatin. The gels were washed with renaturing buffer (25% Triton X-100 solution) for 30 min at room temperature, followed by incubation in activation buffer for 30 min and an additional incubation in fresh developing buffer for 15 hours at 37°C. Following incubation, the gels were stained for 1 hour in a solution of 2% brilliant blue, 50% ethanol and 10% acetic acid. After bleaching for 30 min in 30% methanol mixed with 10% acetic acid, the gels were fixed in distilled water. The density of each lytic band was measured using

a 2020 Ultrascan Laser Densitometer (LKB, Sweden).

(C) Flow cytometry analysis of peripheral blood cells

To characterize the phenotypes of bone marrow derived stem cell in peripheral blood, flow cytometric analysis was performed. Whole blood was collected at 24 hours and 48 hours postoperatively and treated with 0.05% trypsin and 0.53 mM ethylenediamine tetraacetic acid (EDTA) and washed twice with PBS. Cell aliquots (1×10^6 cells/mL of PBS) were stained with primary antibodies at room temperature for 30 minutes.

The primary antibodies were fluorescein isothiocyanate-conjugated anti-CD34(#7324, Santa Cruz, CA, USA), VEGFR2(ab2349, Abcam, Cambridge, Mass., USA), and CD133 (MAB4310, Chemicon, Temecula, CA, USA). Flow cytometry was performed on a fluorescence-activated cell sorter (FACS Calibur, BD Biosciences), and data analysis was performed using Cell Quest software (BD Biosciences).

6. Measurement of survival area of flaps and blood flow

(A) Evaluation of survival area of flaps

Flap survival area was measured using digital photo analysis. The colors of digital images obtained at a constant exposure and distance were converted into numerical values. Survival area was defined as the difference between the total area and the demarcated area of necrosis. Survival rate was defined as a percentage by dividing the survival area by the total area. At postoperative day

7, the survival areas over time were compared quantitatively by comparing the digital images obtained from experimental and control groups. The length of each image was converted into the actual length utilizing ImageJ[®] software (NIH-Scion Corporation, Bethesda, MD, USA).

(B) Physiologic assessment of blood flow by laser Doppler

At postoperative day 7, laser Doppler (Periflux system 5000[®], Perimed AB, Jarfalla, Sweden) located 2 cm proximal to the base of the flap was used to investigate the variation of blood flow. Rats were anesthetized with with zolazepam-tiletamine mixture (Zoletil[®], Virbac, Carrs, France) and an average value for blood flow was calculated from three measurements per rat and recorded as perfusion unit. By placing a probe perpendicular to the flap, it is monitored continuously for 10 seconds during each measurement.

7. Histology

(A) Quantitative measurement of vascularization

Seven days after flap elevation, segments of tissue (0.5cm x 1.0cm) were obtained from an area 3cm away from the base of the flap along the long axis. The skin tissue was embedded in paraffin and 5 μ m sections were obtained. Both hematoxylin and eosin staining and immunohistochemical staining for CD31 (anti-CD31 antibody, #1506, Santa Cruz, CA, USA) were performed. Capillaries were observed as a single layer of flattened endothelial cells without smooth muscle, as observed at 200X on an optical microscope (Olympus,

Tokyo, Japan). To eliminate bias, capillaries were counted in eight areas (0.46 mm²) by an independent researcher blinded to the treatment group, and the capillary density was recorded as capillary count/mm².

(B) Measurement of expressions of VEGF, SDF-1, and HIF-1 α in tissue

Both hematoxylin and eosin staining and immunohistochemical staining for VEGF (anti-VEGF, #7269, Santa Cruz, CA, USA), SDF-1 (anti-SDF1, #3740S, CST, Danvers, MA, USA) and HIF-1 α (anti-HIF-1 α , #53546, Santa Cruz, CA, USA) were performed on flap tissue. Expression levels of VEGF, SDF-1 and HIF-1 α were analyzed by immunohistochemistry using imaging analysis software (Metamorph[®], Universal Imaging Corporation, Downingtown, PA, USA).

8. Western blot analysis

Western blotting was used to analyze factors that play key roles in vasculogenesis and angiogenesis, including VEGF (anti-VEGF, #7269, Santa Cruz, CA, USA), HIF-1 α (anti- HIF-1 α , #53546, Santa Cruz, CA, USA) and SDF-1 (anti-SDF-1, #3740S, CST, Danvers, MA, USA). At 7 days after flap elevation, segments of tissue (0.5cm x 1.0cm) were obtained from an area 3cm away from the flap base along the long axis. Tissues were washed with PBS and centrifuged at 3,000 rpm for 2 min, dissolved in RIPA buffer (10mM PBS, 1% NP40, 0.5% sodium deoxycholate and 0.1% SDS) containing proteinase inhibitors (10 ml/ml PMSF, 30 ml/ml aprotinin [cat # A6279, Sigma, St. Louis,

MO, USA] and 10 ml/ml sodium orthovanadate [100 mM]). The obtained samples were treated with electrophoresis loading buffer (1.0 ml glycerol, 0.5 ml 2-mercaptoethanol, 3.0 ml 10% SDS, 1.25 ml 1.0M Tris-HCL [pH 6.7], 1-2 mg bromophenol blue) and simmered for 3 minutes. 10% SDS-PAGE electrophoresis was performed on nitrocellulose membranes (Millipore Co., Bedford, MA, USA). Membranes were blocked with 10mM Tris-buffered saline (TBS, pH 8.0) containing 5% nonfat dry milk at 4°C overnight. It was treated with anti-rabbit as 1:1,000 diluted secondary antibody and anti-goat (Amersham, Arlington Heights, Ill, UK) for 1 hr. Then, membranes were detected radiographically using Amersham Hyperfilm ECL (Amersham, Arlington Heights, Ill, UK). Chromophores from the ECL system (Amersham, UK) VEGF concentrations were normalized by β -actin. Concentrations of SDF-1 and HIF1- α were normalized by Glyceraldehyde-3-phosphate dehydrogenase(GADPH). Relative protein expression was determined using Image J[®] software (NIH-Scion Corporation, Bethesda, MD, USA).

9. Quantitative real-time reverse transcriptase polymerase chain reaction (RT-PCR)

We used RT-PCR to analyze the experimental genes for vascular endothelial growth factor A (VEGFA), vascular endothelial growth factor Receptor 2 (VEGFR2, Flk-1/KDR), endothelial nitric oxide synthase 3 (NOS3, eNOS), stromal cell-derived factor 1 α (SDF-1, CXCL12) and hypoxia-inducible factor-

1 (HIF-1 α). Total RNA was prepared with TRIzol™ Reagent (Invitrogen, Carlsbad, CA, USA), and complementary DNA was prepared from 0.5 μ g of total RNA by random priming using a first-strand cDNA synthesis kit (Promega, Fitchburg, WI, USA), under the following conditions: 95°C for 5 minutes, 37°C for 2 hours, and 75°C for 15 minutes.

Quantification of mRNA was performed using SYBR green on cycler. TaqMan® primer/probe kits were used to analyze mRNA expression levels by use of an ABI Prism 7500 HT Sequence Detection System (Applied Biosystems, Foster City, CA, USA). Target mRNA levels were measured relative to an internal mouse beta actin (ACTB) control. For cDNA amplification, AmpliTaq Gold® DNA polymerase was activated by incubating for 10 minutes at 95°C; this was followed by 40 cycles of 95°C for 15 seconds and 60°C for one minute per cycle. To measure cDNA levels, the threshold cycle at which fluorescence was first detected above baseline was used, and a standard curve was drawn between the starting nucleic acid concentrations and the threshold cycle. The mRNA expression levels were normalized to the levels of ACTB, and then relative quantification was expressed as fold-induction compared with control conditions (group I). The relative mRNA expression levels were calculated according to the comparative Ct($\Delta\Delta$ Ct) method (Applied Biosystems).²¹ The target quantity was normalized to an endogenous control and relative to a calibrator, and was calculated using formal: target amount = $2^{-\Delta\Delta C_t}$.

10. Statistical analysis

All data obtained were analyzed with SPSS version 18.0 statistical software (SPSS, Inc., Chicago, Ill, USA) and verification was performed by the Kruskal-Wallis test and the Mann-Whitney test. Tests were significant at $p < 0.05$.

III. RESULTS

1. Selection of the optimal dosage and injection route for AMD-3100

The association of survival rate of flaps and concentration of AMD-3100 was statistically significant. The flap survival rate was highest (85.1%) for injection of 10mg/kg AMD-3100. ($p<0.05$, Kruskal-Wallis test, Table 3, Figure 3). The flap survival rates were 68.7% and 79.7% for injection of PBS and 5mg/kg AMD-3100, respectively.

The association of survival rate of flaps injection route of AMD-3100 was also statistically significant. Subcutaneous injection yielded a higher survival rate compared with that of intraperitoneal and intravenous injection ($p<0.05$, Kruskal-Wallis test, Table 4, Figure 3).

Table 3. Survival rate of flaps (%) according to the concentration of AMD-3100

Group	Median (min~max)(%)	<i>p</i> -value
PBS	68.7 (65.6~74.2)	
AMD-3100 5mg/kg	79.7 (65.9~89.5)	
AMD-3100 10mg/kg	85.1 (71.2~95.3)	0.003*

* $P<0.05$, Kruskal-Wallis test

Table 4. Survival rate of flaps according to injection route of AMD-3100

Group	Median (min~max), %	<i>p</i> -value
5mg/kg SC	85.2 (78.6~89.5)	<0.001*
5mg/kg IV	71.3 (65.9~76.2)	
5mg/kg IP	81.3 (76.8~86.6)	
10mg/kg SC	93.9 (89.6~95.3)	<0.001*
10mg/kg IV	74.0 (71.2~79.6)	
10mg/kg IP	89.2 (87.5~93.2)	

* *P*<0.05, Kruskal-Wallis test
SC:subcutaneous, IV:intravenous, IP:intraperitoneal

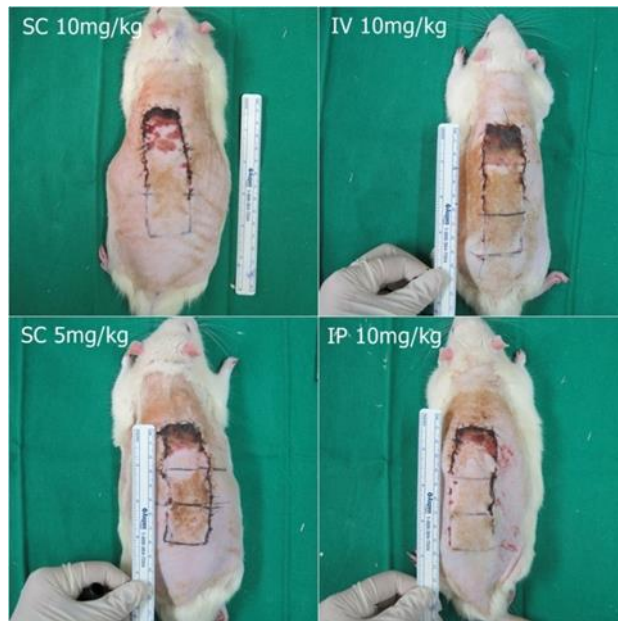


Figure 3. Survival of flaps according to dosage of AMD-3100

Injection of 10mg/kg AMD-3100 through subcutaneous route yields highest survival rate.

2. Differentiation and mobilization of EPC from bone marrow hematopoietic stem cells following injection of AMD-3100

(A) Gelatin zymography for active MMP-9 in bone marrow

As shown by zymography, there were significantly higher levels of active MMP-9 in bone marrow from rats injected with AMD-3100 (groups III and IV) as compared to rats injected with PBS (groups I and II) at postoperative day 2 ($p=0.045$, Mann-Whitney test, Figure 4). However, the mean value of active MMP-9 in bone marrow from rats in group III was not statistically significantly higher than that of rats from group IV.

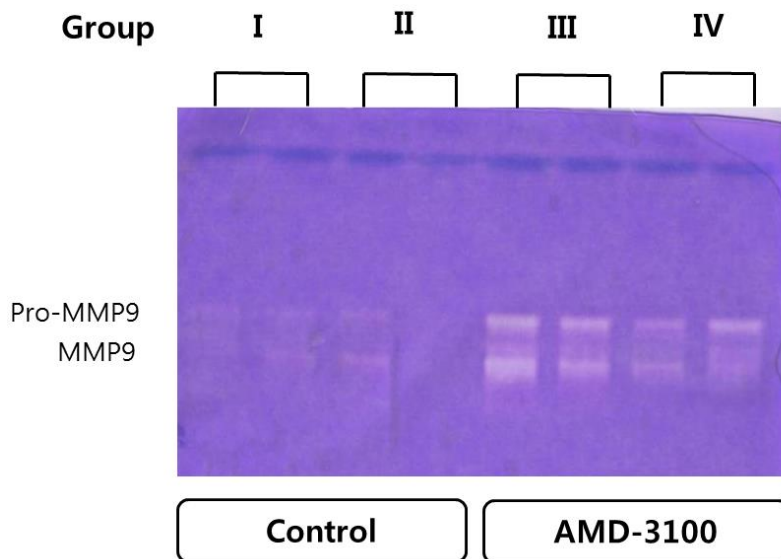


Figure 4. MMP-9 zymography.

(B) Flow cytometry analysis of peripheral blood cells

The fraction of VEGFR2+ cells in the peripheral blood of rats in Group III was significantly higher than any other group on days 1 and 2 after the procedure ($p < 0.05$, Kruskal-Wallis test). On the same days, the fraction of VEGFR2+/CD34+ double-positive cells in the peripheral blood of rats from group IV (AMD-3100, expanded) was statistically significantly higher than any other group. ($p < 0.05$, Kruskal-Wallis test, Figures 5, 6, 7) Flow cytometric analysis showed that there were few CD133 positive cells in peripheral blood of all groups, regardless of treatment with AMD 3100.

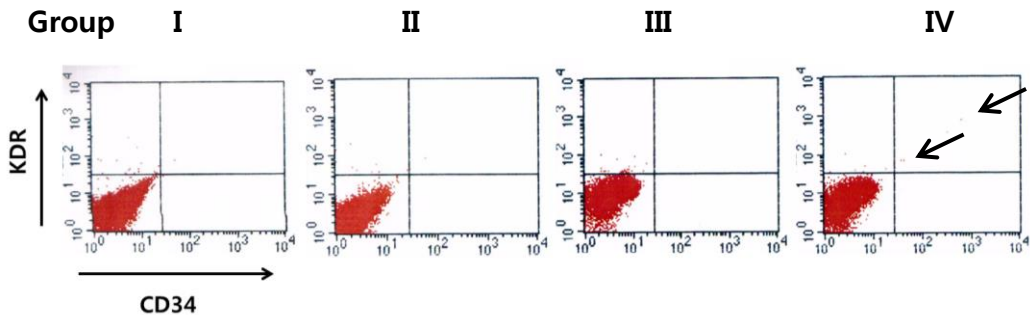


Figure 5. Fraction patterns of CD34/VEGFR2 cells. The expression of surface markers VEGFR2 and CD34 was analyzed in peripheral blood cells by flow cytometry. Quadrants were set on the basis of isotype controls. Arrows indicate CD34⁺/VEGF2R⁺ double-positive cells.

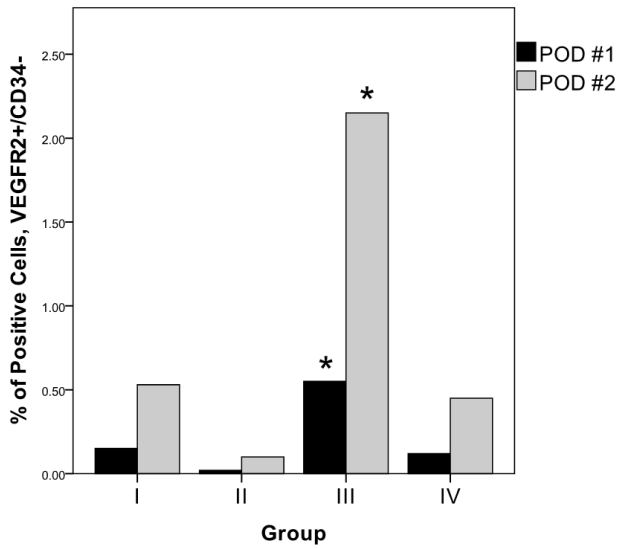


Figure 6. Fraction pattern of VEGFR2+ cells in peripheral blood (* $p < 0.05$, Kruskal-Wallis test)

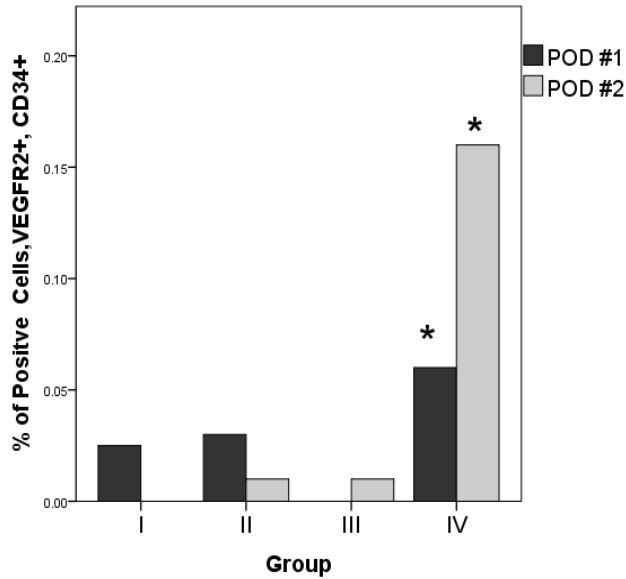


Figure 7. Fraction pattern of double-positive VEGFR2+/CD34+ cells in peripheral blood (* $p < 0.05$, Kruskal-Wallis test)

3. Survival area of flaps

(A) Preliminary study of survival rate in unexpanded flaps

In rats treated with AMD-3100 and without a silicone sheet, the median survival rate of classical unexpanded flaps (group C) was 94%. This was significantly different from the survival rate of flaps in control rats (group A, no AMD-3100 treatment, no silicone sheet) at postoperative day 7 ($p=0.004$, Mann-Whitney test, Figures 8, 9A and Table 5). When a silicone sheet was added, the median survival rate was also significantly higher in rats treated with AMD-3100 (group B) than in rats without treatment (group B vs. group D, $p=0.002$, Figures 8, 9A, Table 5).

Insertion of a silicone sheet under the flap significantly decreased the median survival rate compared with flaps in without the silicone sheet (p (group A and B)=0.011, p (group C and D)=0.017), regardless of injection of AMD 3100 (Figure 9B).

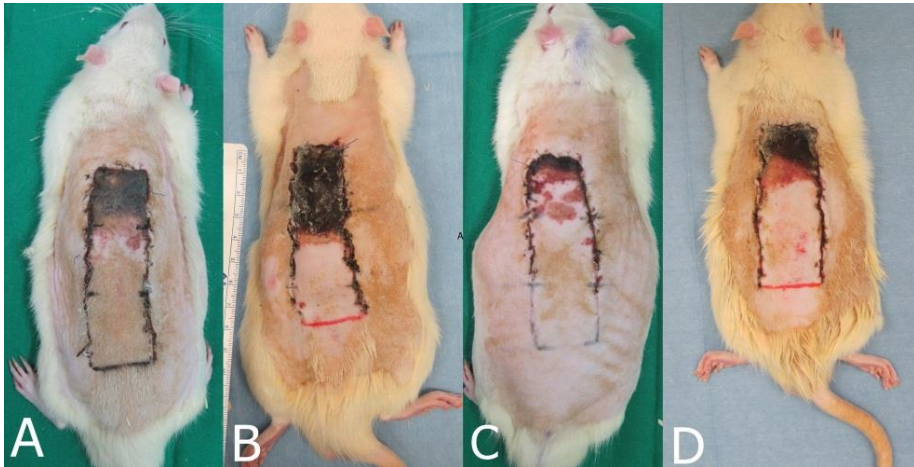


Figure 8. Photographs depicting flap survival in the preliminary study of unexpanded flaps

(A) Group A, control without silicone sheet; (B) Group B, control with silicone sheet; (C) Group C, AMD-3100 injection without silicone sheet; (D) Group D, AMD-3100 injection with silicone sheet.

Table 5. Survival rate of flaps in the preliminary study of unexpanded flaps

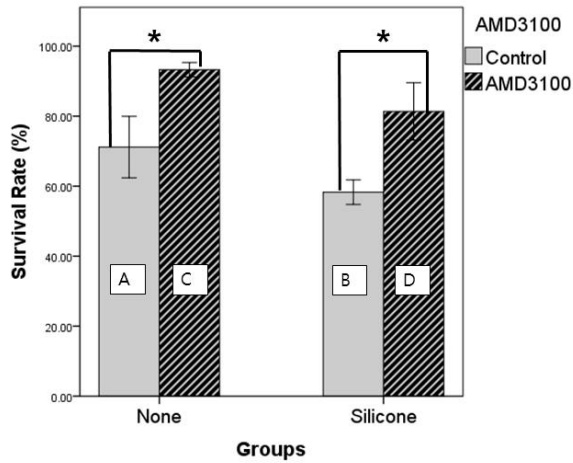
Group	Median (min~max)(%)	<i>p</i> -value
A (control)	69 (65~82)	
B	59 (53~64)	0.011*
C	94 (89.6~95.39)	<0.0001*
D	85 (71~95.3)	0.127
†A vs. C		0.004*
†B vs. D		0.002*
†C vs. D		0.017*

* $P < 0.05$, Mann-Whitney test between control and other groups

†Mann-Whitney test between groups

(A) Group A, control without silicone sheet; (B) Group B, control with silicone sheet; (C) Group C, AMD-3100 injection without silicone sheet; (D) Group D, AMD-3100 injection with silicone sheet.

A



B

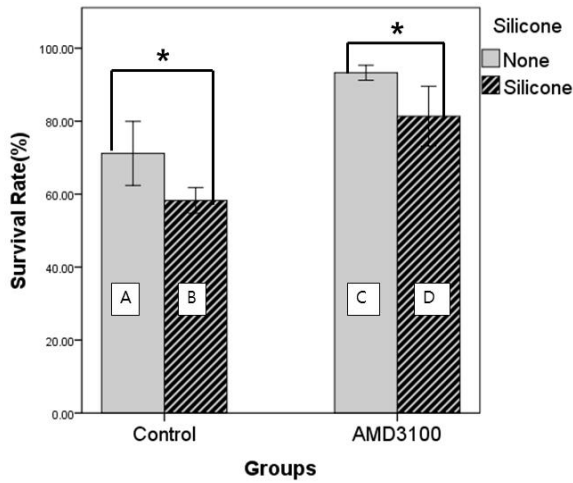


Figure 9. Survival rates of flaps in the preliminary study of unexpanded flaps. (A) Treatment with AMD-3100 significantly increased survival rates in classical unexpanded flaps, with or without insertion of a silicone sheet. (B) Insertion of a silicone sheet under the flap blocked the blood supply from the bed. In a classical unexpanded flap, the mean survival rate of flaps without insertion of a silicone sheet was greater than flaps with a silicone sheet, regardless of treatment with AMD-3100 (* $p < 0.05$, Mann-Whitney test).

(B) Main study of survival rate in expanded flaps

The survival rates (% , median) of flaps for group I, group II, group III and group IV were 59%, 50%, 61% and 51.5%, respectively, at postoperative day 7. However, the survival rate of flaps in group I (untreated, unexpanded) was not significantly different from the other groups ($p>0.05$, Kruskal-Wallis test, Figures 10, 11A, Table 6).

The survival rate of flaps in rats treated with AMD-3100 (group III and IV) was not significantly different than of flaps in untreated rats (group I and II, $p=0.443$, Mann-Whitney test, Table 6, Figure 11A). However, the survival rate of flaps for group III (treated with AMD-3100, unexpanded) was significantly higher than that for group IV (treated with AMD-3100, expanded, $p=0.0029$, Mann-Whitney test, Table 6, Figure 11B). The survival rate (% , median) of unexpanded flaps (groups I and III) was significantly higher than the survival rate of expanded flaps (group II and IV, $p=0.004$, Mann-Whitney test).

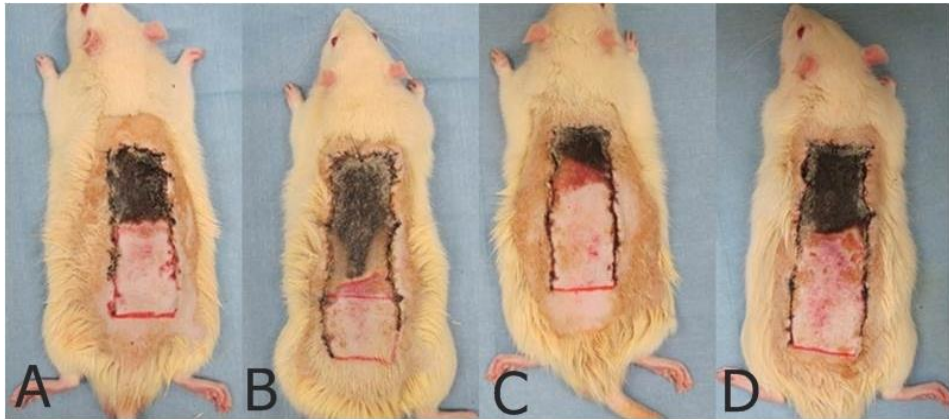


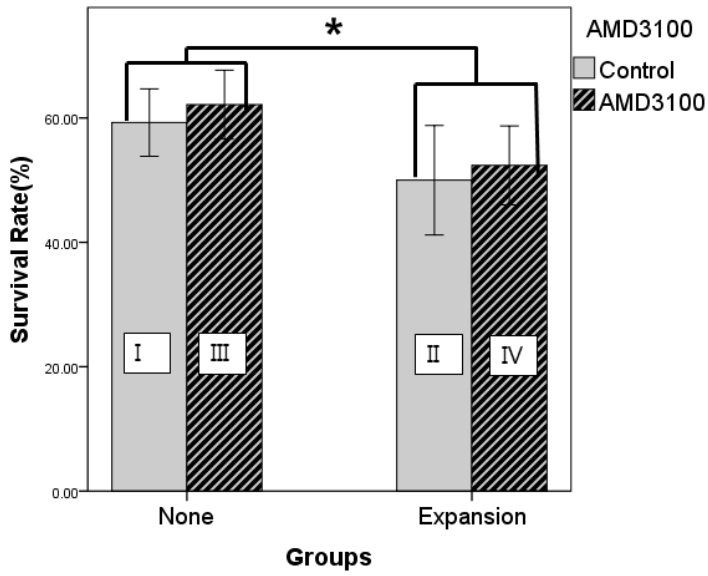
Figure 10. Photographs depicting flap survival in the main study
(A) Group I; (B) Group II; (C) Group III; (D) Group IV.

Table 6. Survival rate of flaps in the main study

Group	Median (min~max)(%)	<i>p</i> -value
Group I	59 (52.8~64)	
Group II	50 (53~64)	0.082
Group III	61 (56~74)	0.530
Group IV	51.5 (42~63)	0.127
†II vs. IV		0.573
†III vs. IV		0.029*
†No expansion(I and III) vs. Expansion (II and IV)		0.004*
†Control (I and II) vs. AMD-3100 (III and IV)		0.443

Mann-Whitney test between group I and other groups (II, III, and IV)
†Mann-Whitney test between groups
* $P < 0.05$, Mann-Whitney test

A



B

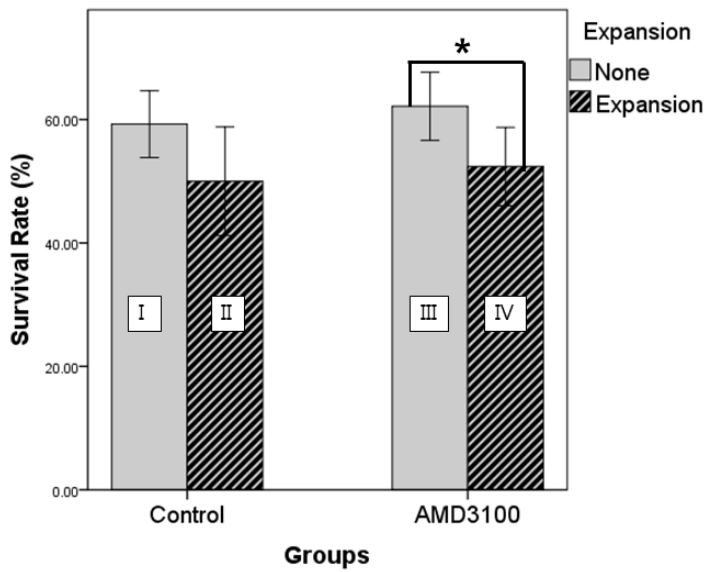


Figure 11. Survival rate of flaps in the main study
(* $p < 0.05$, Mann-Whitney test)

4. Physiologic assessment of blood flow by laser Doppler

At postoperative day 7, blood flow measured by laser Doppler in the proximal portion of the flaps was not significantly different between the groups ($p>0.05$, Kruskal-Wallis test, Table 7).

Table 7. Blood flow measured by laser Doppler

Group	Median (min-max)	<i>p</i> -value
Group I	38 (33~52)	0.534
Group II	22 (22~42)	
Group III	23 (18~54)	
Group IV	22 (14~67)	

P<0.05, Kruskal-Wallis test

5. Histology

(A) Quantitative measurement of vascularization

At postoperative day 7, groups III and IV (treated with AMD-3100) showed a statistically significant increase in vessel area compared with groups I and II (untreated). However, there was no significant difference in the area of vessels between groups I and II or between groups III and IV. In the same manner, group III and IV showed a statistically significant increase in vessel number compared with groups I and II. However, there was no significant difference in the area of vessels between groups I and II or between group III and IV (Table 8, Figure 12, 13, $p<0.05$, Mann-Whitney test).

Table 8. Vessel area and vessel number

Vessel Area			
Group	Relative surface area		<i>p</i> -value
	Median (Range)		
Group I	13139	(3707~28046)	
Group II	18614	(3269~61029)	0.244
Group III	20740	(943~53457)	<0.0001*
Group IV	24893	(8309~111780)	0.001*
* <i>p</i> <0.05, Mann-Whitney test compared with group I			
II vs. III			<0.0001*
II vs. IV			<0.0001*
III vs. IV			0.326
* <i>p</i> <0.05, Mann-Whitney test compared between groups			
Vessel Counts			
Group	Numbers		<i>p</i> -value
	Median (Range)		
Group I	581	(191 ~709)	
Group II	593	(275~1144)	0.110
Group III	1341	(107~2197)	<0.0001*
Group IV	924	(590~3030)	0.001*
* <i>p</i> <0.05, Mann-Whitney test compared with group I			
II vs. III			<0.0001*
II vs. IV			<0.0001*
III vs. IV			0.324
* <i>p</i> <0.05, Mann-Whitney test compared between groups			

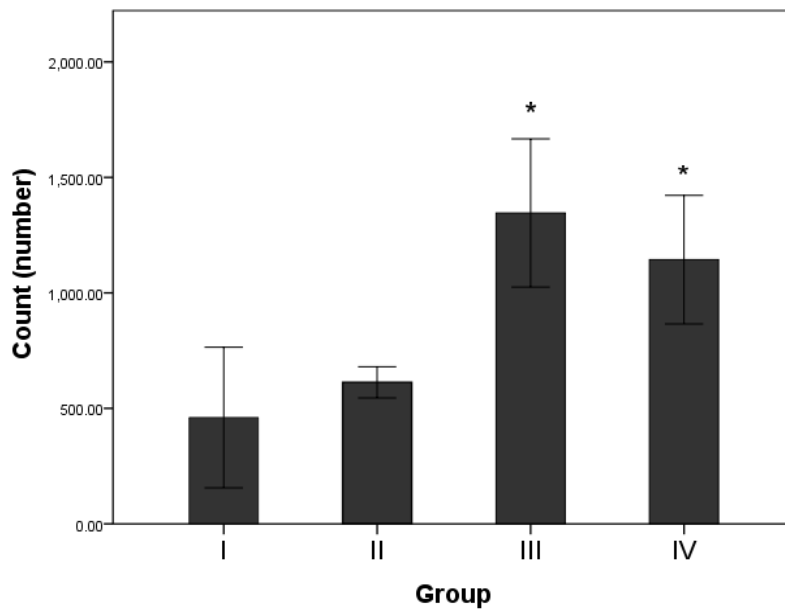
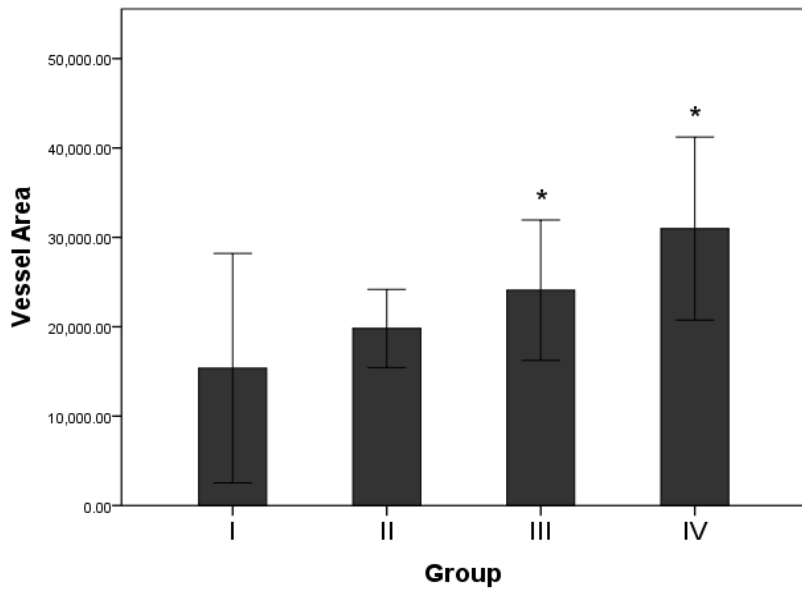


Figure 12. Vessel areas and counts by immunohistochemical staining for CD31.

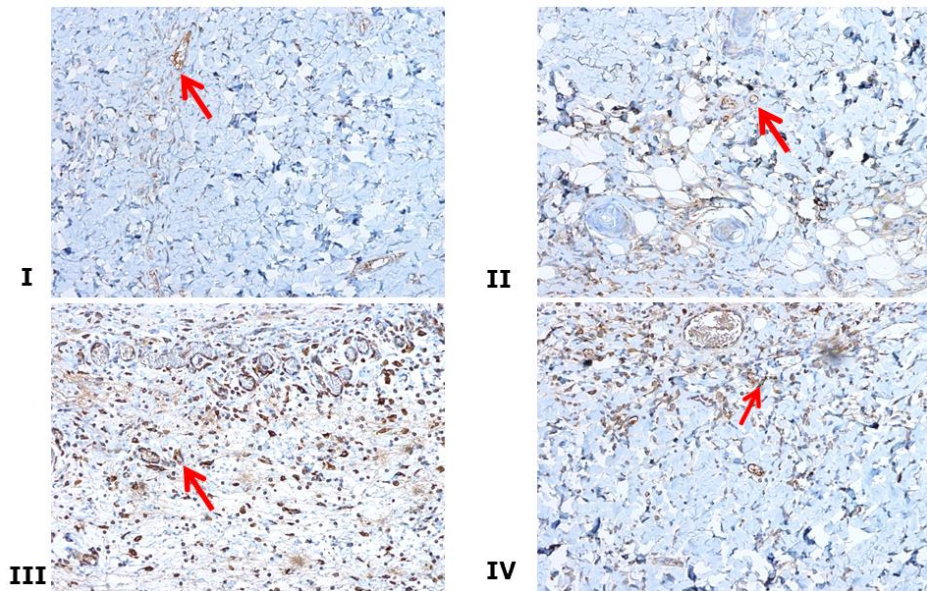


Figure 13. Immunohistochemical staining for CD-31. (200X)
 Arrows indicate vessels. Group III and IV (received AMD-3100 injection) showed statistically significant increases in vessel number compared with group I (control).

(B) Density of VEGF, SDF-1 and HIF-1 α in tissue flaps

At postoperative day 7, the density of VEGF in the proximal portion of the flaps, as measured by immunohistochemistry and Metamorph[®] software, was significantly different between the groups. Groups II, III and IV showed a significant increase in expression of VEGF compared with group I (Table 9, Figures 14, 15, $p < 0.05$, Mann-Whitney test).

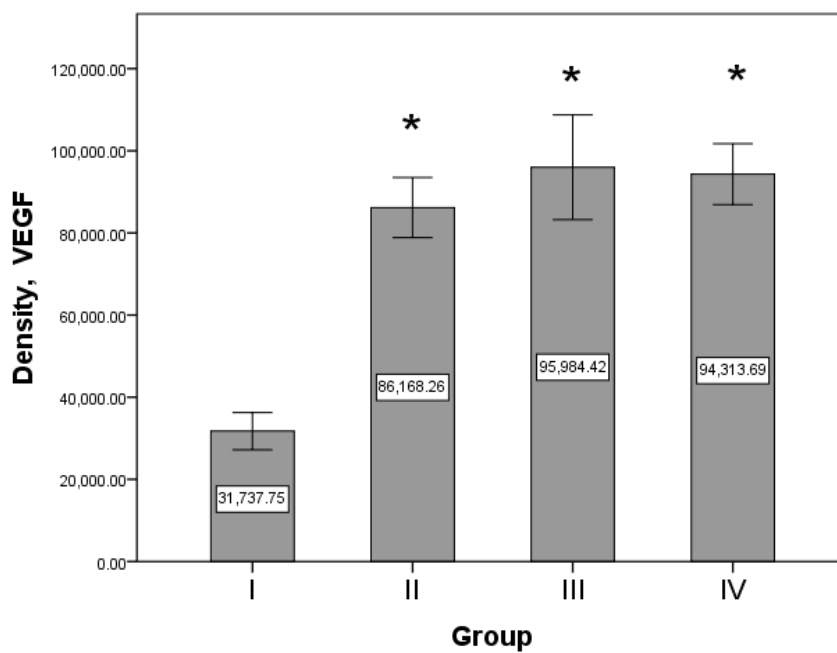


Figure 14. Density of VEGF in flap tissue

Table 9. Density of VEGF

Group	<i>p</i> -value
I vs. II	<0.0001*
I vs. III	<0.0001*
I vs. IV	<0.0001*
II vs. III	0.218
II vs. IV	0.126
III vs. IV	0.815

* : $p < 0.05$ in Mann-Whitney test

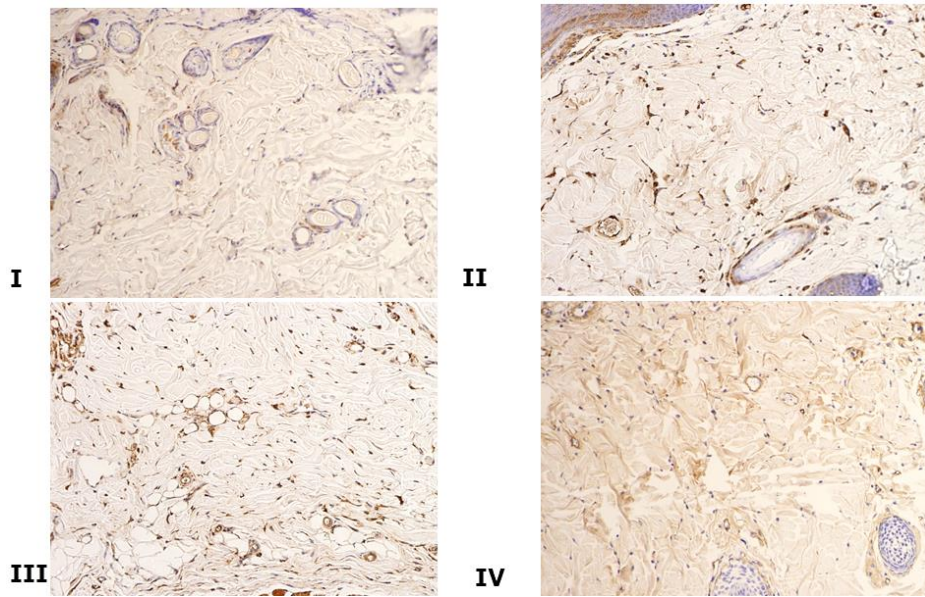


Figure 15. Immunohistochemical staining for VEGF. (200X)

At postoperative day 7, the density of SDF-1 and HIF-1 α in the proximal portion of the flaps, as measured by immunohistochemical staining and Metamorph® software, was not significantly different between the groups ($p > 0.05$, Kruskal-Wallis test, Figures 16,17).

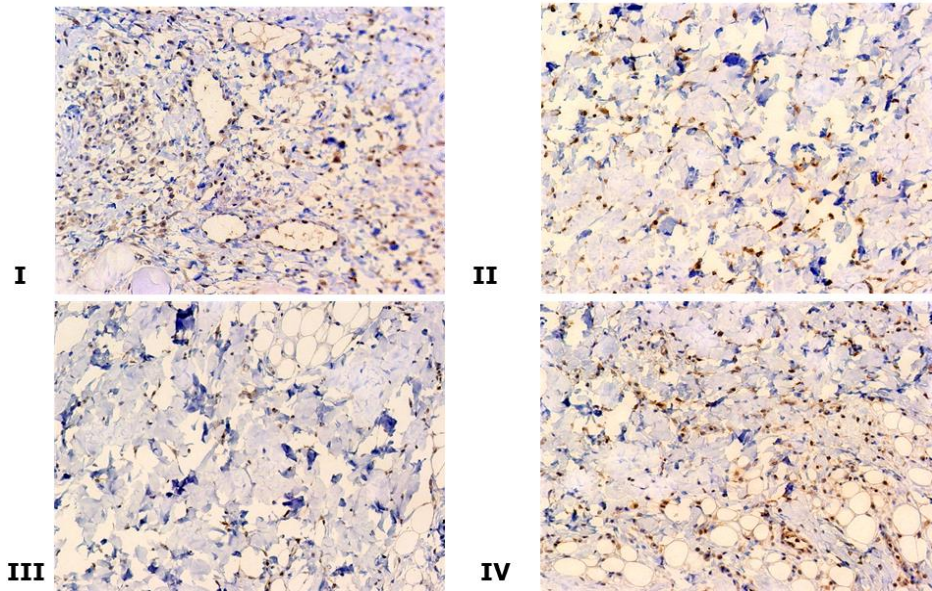


Figure 16. Immunohistochemical staining for SDF-1. (200X)

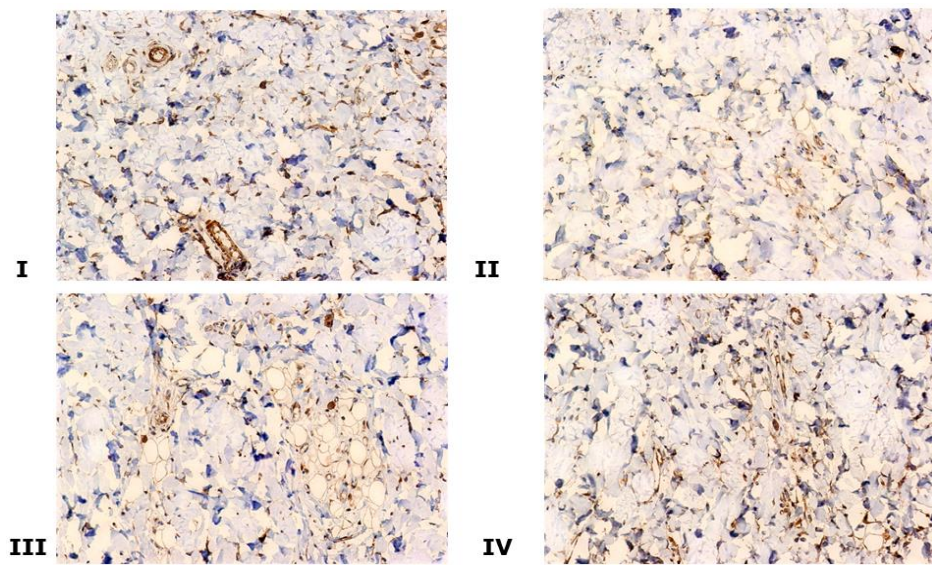


Figure 17. Immunohistochemical staining for HIF-1 α . (200X)

6. Western blot analysis

At postoperative day 7, Western blot analysis of VEGF, SDF-1 and HIF-1 α in the proximal portion of the flaps showed no significant differences between groups ($p > 0.05$, Kruskal-Wallis test, Figures 18, 19, 20).

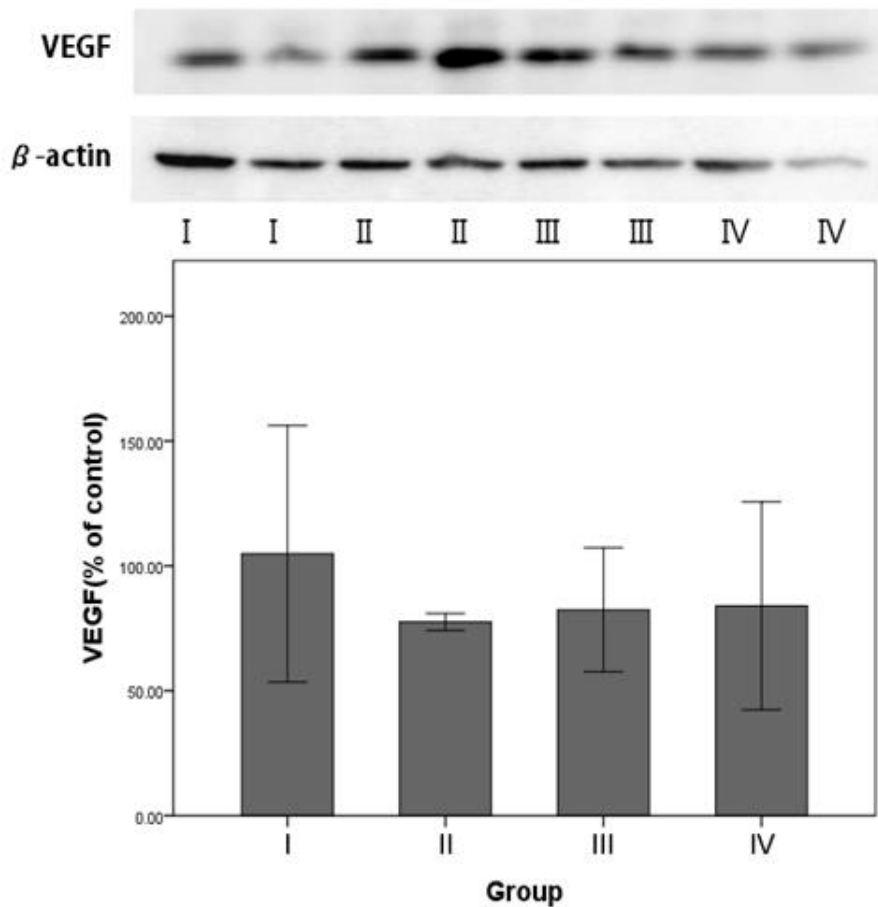


Figure 18. Western blot analysis of VEGF

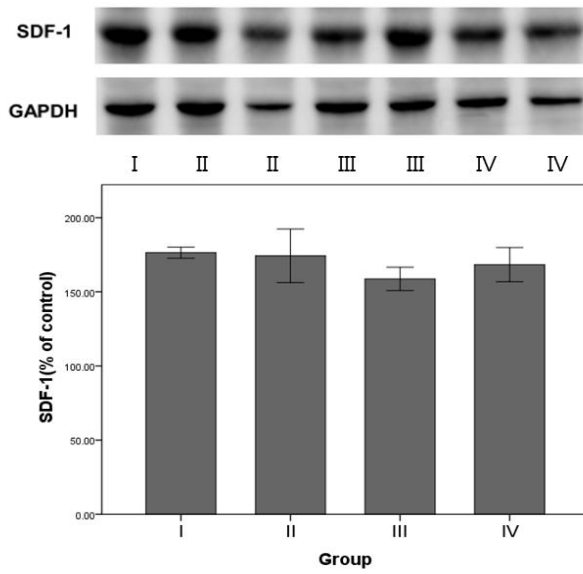


Figure 19. Western blot analysis of SDF-1

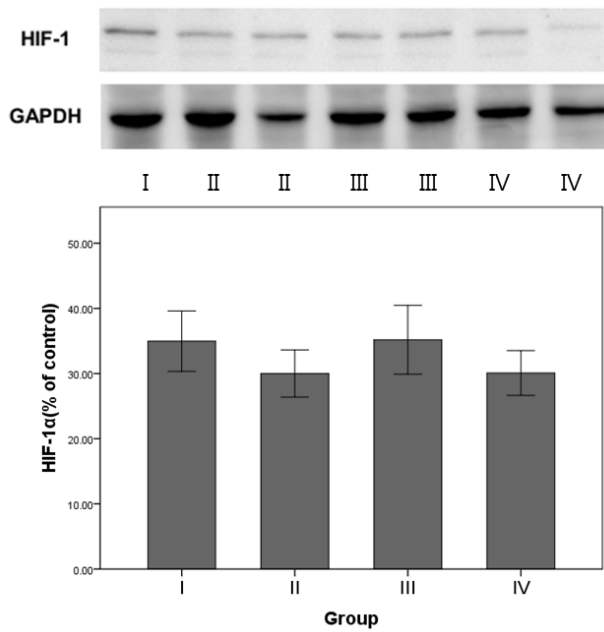


Figure 20. Western blot analysis of HIF-1α

7. Real-time quantitative RT-PCR of VEGFA, VEGFR2, NOS3, SDF-1 and HIF-1 α

RT-PCR was used to measure the change in levels of selected genes in the proximal portion of the flaps at postoperative day 7. The “fold change” in the gene for VEGFA was significantly increased in group II (1.5 ± 0.3 , $p=0.048$), group III (12.3 ± 15.5 , $p=0.024$) and group IV (15.1 ± 2.7 , $p=0.048$) compared to group I (control). The fold-change in the gene for VEGFR2 was significantly increased in group III (1.2 ± 0.3 , $p=0.024$), but there was no change in the VEGFR2 gene in group II or group IV. The expression of the gene for SDF-1 was significantly increased in group III (1.3 ± 0.6 , $p=0.024$), but there were no significant changes in the SDF-1 gene in group II or group IV. The genes for NOS3 and HIF-1 α were not significantly different between groups (Figure 21).

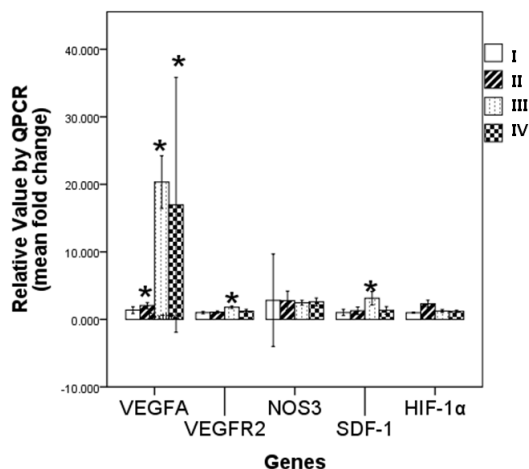


Figure 21. Real time quantitative RT-PCR measurement of VEGFA, VEGFR2, NOS3, SDF-1 and HIF-1 α . * $p < 0.05$, Significant difference compared with control levels (group I) by Mann-Whitney test.

IV. DISCUSSION

Tissue flaps used for reconstruction of soft tissue defects must survive ischemic conditions by increasing vasculogenesis and angiogenesis at the flap itself and between the flap and the recipient site. For effective reconstruction using a tissue flap, the flap should have a larger survivable area with a smaller diameter pedicle, in order to reduce the morbidity of donor site. Gradual repeated tissue expansion at the donor site, which is going to be the flap, allows for greater neovascularization and regeneration of new skin by hypoxic and mechanical stimuli. This procedure has the advantage of expanding the survivable area of the donor flap despite the limited size of the donor tissue.²²

The most potent stimulus for neovascularization is hypoxia, which induces new blood vessel growth in order to restore adequate oxygen delivery to the ischemic tissue.^{15,23} EPCs participate in neo-vascularization under ischemic conditions.^{23,24} The ability of EPCs, but not mature endothelial cells, to proliferate in severely hypoxic conditions suggests a pivotal role for EPCs as the major building block for new vessels in ischemic tissues.^{23,25} The gradient of hypoxia/ischemia ultimately directs EPCs to coalesce into independent vascular structures in order to restore tissue perfusion in the ischemic region.²³ This gradient of hypoxia is established in both the classical caudally based dorsal skin flap and in the experimental expanded flap model. Tissue expansion, as in the expanded flap model, and vacuum assisted closure more effectively create the gradient of hypoxia surrounding the lesion during continuous expansion.²⁶

A disadvantage of the tissue expansion technique in large soft tissue defects, which require a long expansion time, is the inherent limit of the ability of the skin and soft tissue to regenerate.²⁷ To address this concern, many methods have been reported to increase the efficacy of tissue expansion, such as intraoperative acute skin stretching,²⁸ transplanting bone marrow derived stem cells,²⁷ and making use of compounds such as botulinum toxin,²⁹ papaverine,³⁰ dimethyl sulfoxide,³¹ and verapamil.³² Intermittent intraoperative skin stretching has been shown to improve flap viability by up-regulating VEGF and VEGFR2 at postoperative day 2 and decreasing necrosis by 50-75% at postoperative day 5.^{28,33} In order to increase the viability of tissue in expanded flaps and the efficacy of tissue expansion, it might be possible to enhance the recruitment of EPCs for vasculogenesis, increase VEGF concentration to induce angiogenesis, and create more favorable interactions with EPCs as a chemotactic factor.

Pretreatment of mice with G-CSF prior to administration of AMD-3100 has been shown to dramatically increase the mobilization of hematopoietic stem cells and neutrophils, but not EPCs, to the peripheral blood from the bone marrow. Pretreatment of mice with VEGF prior to administration of AMD-3100 has been shown to reduce the release of hematopoietic stem cells and leukocytes into the peripheral blood but to increase the mobilization of EPCs and mesenchymal stem cells.^{18,19} Mobilization of EPCs is mediated by MMP-9 and regulated by hypoxic gradients through HIF-1 α -inducted SDF-1(CXCL12) in the bone marrow.^{14,34} It has been reported that, immediately following a

myocardial infarction (MI), acute antagonism of CXCR4 induced by AMD-3100 increases the number of EPCs in the peripheral blood for 1-2 weeks, improves survival and increases capillary density.³⁵ AMD-3100-induced MMP-9 expression is mediated via VEGF.³⁵ VEGFR2 increases as early as 2 hours after stretching and expression levels of these receptors return to the levels of non-stretched skin at day 7.³⁶

In this study, the fraction of EPCs (VEGFR2+/CD34+ double positive cells) was highest in group IV (expanded flaps, treated with AMD-3100), which might have the most continuous ischemic conditions at postoperative day 2. The fraction of single positive VEGFR2+ cells in the peripheral blood in group III (not expanded, treated with AMD-3100) significantly increased at postoperative day 2. The expression levels of MMP-9 in the bone marrow and the fraction of EPCs in peripheral blood were both significantly increased the groups that received AMD-3100 (III and IV) in comparison with the groups that did not receive AMD-3100 (I and II). These results suggest that AMD-3100 contributes to the effective endogenous mobilization and differentiation of bone marrow derived hematopoietic stem cells to the peripheral blood in response to ischemic conditions of flaps by increasing VEGFR2-positive cells and EPCs (VEGFR2/CD34 double positive cells) in the peripheral blood. Furthermore, bone marrow derived stem cells might differentiate according to the level of ischemia of the flap in the presence of AMD-3100.

To investigate the condition of the microenvironment under expansion and

AMD-3100, we harvested the proximal tissues of flaps and analyzed these tissues by immunohistochemistry, Western blotting and real-time quantitative RT-PCR to detect VEGFA, VEGFR2, SDF-1, NOS-3 and HIF-1 α .

The expression levels of VEGF in groups II, III and IV, as measured by immunohistochemistry (Figure 14) and real-time quantitative RT-PCR (Figure 21), were statistically significantly higher than in group I at postoperative day 7. These results suggest that AMD-3100 and tissue expansion may play a favorable role in increasing VEGF. SDF-1 and VEGFR2 in the classical unexpanded flap treated with AMD-3100 were expressed at statistically significantly higher levels than in group I (control,) as measured by real-time quantitative RT-PCR (Figure 21). This might be correlated with the result of flow cytometry analysis showing that the fraction of VEGFR2 positive cells in the peripheral blood was higher than other group at postoperative day 2 (Figure 5). VEGF and SDF-1 have been known to have direct and indirect effects on EPCs in a neovascularization system, including recruitment of EPCs from the bone marrow into the blood circulation by an MMP-9-dependent mechanism, homing and proliferation of EPCs, and incorporation into new vessels.^{35,37} EPCs also mediate the release of VEGF and SDF-1 at the ischemic lesion, in a paracrine fashion.³⁸

NOS3 enzymatically generates nitric oxide (NO) in endothelial cells and regulates vascular functions such as smooth muscle relaxation and vasodilation. NOS3 may stimulate neovascularization due to VEGF, although enhancement

of ischemia-induced angiogenesis by eNOS overexpression is not dependent on VEGF.^{39,40} In our studies, there was no difference in the level of expression of HIF-1 α and NOS3 between groups at postoperative day 7 (Figure 21). This suggests that the severity of ischemia may be similar between the flaps, regardless of whether or not the flaps were expanded. Although VEGFA was highly expressed in group II, group III, and group IV, the constant expression level of NOS3 in different groups may not affect the vascular function or the neovascularization of the flaps.

Vessel area and the number of vessels in the proximal flaps at postoperative day 7 were increased in rats treated with AMD-3100 compared with flaps from untreated rats, regardless of whether or not the flaps were expanded (Table 8, Figures 12, 13).

Although treatment with AMD-3100 increased neovascularization at ischemic flaps, it didn't affect the survival of ischemic flaps if there was a silicone sheet under the flap or the physiologic blood flow as measured by laser Doppler system. In some experiments, a thin silicone sheet was inserted under the classical dorsal skin flap in the rat model in order to permit the unidirectional caudally based blood flow. With the silicone sheets in place, the survival area of the flap was measured while blocking the vessel formation from the recipient bed. However, flaps with the same shape and pattern of blood flow (without inserting the silicone sheet) have similar survival areas to the general clinical situation. Therefore, the purpose of preliminary study was to evaluate the effect

AMD-3100 while blocking the vasculogenesis and angiogenesis from the recipient. This preliminary study showed that antagonism of CXCR4 induced by AMD-3100 improved flap survival by 94% without the insertion of a silicone sheet. On the other hand, in rats treated with AMD-3100 and using the classical unexpanded dorsal skin flap with the adoption of a silicone sheet under the flap to allow only one-way blood perfusion from the proximal pedicle, flap survival decreased to 85% (Table 5, Figure 9). In the expanded flaps in mice treated with AMD-3100 the survival rate decreased further to 51.5%(Table 6). Although AMD-3100 increases the survival rate of flaps, insertion of a silicone sheet between the flap and the recipient along with tissue expansion might adversely affect the survival of flaps (Figure 11). Expansion may extend the survival area of the flap by increasing the ischemic conditions leading to greater induction of VEGF, but the area of new vessel formation blocked from the bed in expanded flap (5cm x10 cm), was larger than that of unexpanded flap (3cm x 9cm). Therefore, unexpanded flaps treated with AMD-3100 may have a statistically higher level of flap survival than the expanded flap with AMD-3100. Expanded flaps showed a decreased survival rate in comparison with unexpanded flaps, regardless of whether or not they were treated with AMD-3100. This phenomenon also adversely affected the survival of flaps, so that the survival rate of flaps was not statistically significantly different between groups.

In addition to the disadvantage of blocking the neovascularization between flap and recipient site with a silicone sheet, it was assumed that the survival

rate in this main experiment may have been modulated by the systemic condition of the host rats and the requirement for the regeneration of other tissues. The size of our designed flap and silicone implant seemed large and the surgical time required to prepare the flaps was relatively long. Both the increased size of the flap and the increased surgical time are potentially fatal to the rats. Therefore, in these rats, bone marrow derived stem cells may be redirected to play roles in the recovery of organ functions (e.g. heart, liver, kidney), rather than participating in wound healing and tissue regeneration, especially in the expanded flap model.

Most reconstruction methods for soft tissue defects adopt various types of flaps permitting three-dimensional vascularization, with the exception of expanded flaps that use an internal tissue expander. These results suggest that AMD-3100 can effectively rescue the unstable viability of flap and ischemic tissue of recipient site, which is unexpectedly threatened by the wrong design of flap, trauma to pedicle and poor circulation around the flap. Furthermore, in surgery utilizing tissue expansion, only one incision is usually made to insert the tissue expander. Vascularization and tissue regeneration can be further increased by systemic mobilization of EPCs and mesenchymal stem cells in response to the ischemic conditions if the rat is treated with AMD-3100 during expansion.

V. CONCLUSION

In this study, we devised an animal model for an expanded dorsal skin flap and investigated the effects of injection of AMD-3100 on the flap, the mobilization of endogenous bone marrow derived EPCs to the ischemic flap, and the increase in vasculogenesis and angiogenesis at the flap. In this experimental rat model, the mobilization of EPCs from bone marrow to peripheral blood was confirmed by gelatin zymography for active MMP-9 and flow cytometry of EPCs (VEGFR2+/CD34+ double positive cells) and VEGFR2 positive cells. The effects of mobilization of endogenous EPCs and their interaction with the microenvironment at the ischemic lesion were investigated by photometric measurement, flap survival, laser Doppler analysis, histology, Western blotting, and real-time quantitative RT-PCR

1. The level of active MMP-9 was found to be higher in the group of rats that were treated with AMD-3100 than in the group of untreated rats. The fraction of EPCs (VEGFR2+/CD34+ double positive cells) in the peripheral blood was the highest in the group of rats treated with AMD-3100 and with expanded flaps in comparison with the other groups, as demonstrated by flow cytometry. The fraction of VEGFR2+ cells in the peripheral blood in the group of rats that were treated with AMD-3100 and with unexpanded flaps, was statistically significantly increased compared with other groups, suggesting that there was greater mobilization and

differentiation of bone marrow derived hematopoietic stem cells to EPCs in response to ischemia at postoperative day 2.

2. Treatment of AMD-3100 and tissue expansion may have the favorable role to increase VEGF levels in the tissue under ischemic conditions. The constant expression levels of HIF-1 α and NOS3 in flaps from the different groups of rats indicate that the severity of ischemia and vascular function in the flaps did change in any of the groups, regardless of whether or not the rats were treated with AMD-3100 or with flap expansion.
3. AMD-3100 plays a role in the mobilization of endogenous EPCs, and the EPCs have a paracrine effect on the induction of VEGF and SDF-1 at the ischemic area. The expression of VEGF increased due to the development of ischemia in expanded flaps, and there was a greater increase of VEGF in the flaps treated with AMD-3100. The expression of SDF-1 was elevated only in unexpanded flaps that were treated with AMD-3100, which appeared to be dependent on the expression of VEGF.
4. Vessel area and the number of vessels, as measured by immunohistochemistry staining for CD31, were both increased in flaps from rats treated with AMD-3100 in comparison with untreated groups. This suggests that AMD-3100 increases vasculogenesis and angiogenesis in ischemic flaps, regardless of expansion.
5. There was a trend towards a decrease in viability of expanded flaps, regardless of AMD-3100 injection, but an increase in the expression of

VEGF and neovascularization. These results suggest that mobilization of endogenous EPCs may be affected by the vascularity surrounding the flap and that the vital condition of rats with the expanded flap model may cause burden to the rats. To permit vasculogenesis and angiogenesis between a flap and recipient, the survival of flaps may increase when the rats are treated with AMD-3100.

AMD-3100 increases the mobilization of bone marrow derived EPCs to the peripheral blood at the expanded flap, and this mobilization is related to mechanotransductive, pre-hypoxic induction of neovascularization. However, the survival of expanded flaps can be affected by allowing for three dimensional blood flows through neovascularization between a flap and recipient. Survival of flaps can also be affected by the host's vital state through the positive effect of neovascularization by the systemic endogenous modulation of EPCs induced by AMD-3100 injection.

REFERENCES

1. Zuker RM, Filler RM, Lalla R. Intra-abdominal tissue expansion: an adjunct in the separation of conjoined twins. *J Pediatr Surg* 1986;21:1198-200.
2. Gur E, Zuker RM. Complex facial nevi: a surgical algorithm. *Plast Reconstr Surg* 2000;106:25-35.
3. Neumann CG. The expansion of an area of skin by progressive distention of a subcutaneous balloon; use of the method for securing skin for subtotal reconstruction of the ear. *Plast Reconstr Surg* 1957;19:124-30.
4. Radovan C. Breast reconstruction after mastectomy using the temporary expander. *Plast Reconstr Surg* 1982;69:195-208.
5. Austad ED, Rose GL. A Self-Inflating Tissue Expander. *Plast Reconstr Surg* 1982;70:588-94.
6. Codivilla AP, Leonard F. On the Means of Lengthening, in the Lower Limbs, the Muscles and Tissues Which Are Shortened Through Deformity. *Am J Orthop Surg* 1904;2:353-9.
7. Ilizarov GA, Soĭbel'man LM, Chirkova AM. Some roentgenologic and morphologic data on regeneration of bone tissue in experimental distraction epiphysiolysis. *Ortopediia, travmatologiia i protezirovanie* 1970;31:26-30.
8. McCarthy JG, Schreiber J, Karp N, Thorne CH, Grayson BH. Lengthening the human mandible by gradual distraction. *Plast Reconstr Surg* 1992;89:1-8.
9. Morykwas MJ, Argenta LC, Shelton-Brown EL, McGuirt W. Vacuum-assisted closure: a new method for wound control and treatment: animal studies and

- basic foundation. *Ann Plast Surg* 1997;38, 553-62.
10. Takei T, Mills I, Arai K, Sumpio BE. Molecular Basis for Tissue Expansion: Clinical Implications for the Surgeon. *Plast Reconstr Surg* 1998;102:247-58.
 11. Sasaki GH, Pang CY. Pathophysiology of Skin Flaps Raised on Expanded Pig Skin. *Plast Reconstr Surg* 1984;74:66-7.
 12. Cherry GW, Austad E, Pasyk K, McClatchey K, Rohrich RJ. Increased survival and vascularity of random-pattern skin flaps elevated in controlled, expanded skin. *Plast Reconstr Surg* 1983;72:680-7.
 13. Lantieri LA, Martin-Garcia N, Wechsler J, Mitrofanoff M, Raulo Y, Baruch JP. Vascular endothelial growth factor expression in expanded tissue: a possible mechanism of angiogenesis in tissue expansion. *Plast Reconstr Surg* 1998;101:392-8.
 14. Ceradini DJ, Kulkarni AR, Callaghan MJ, Tepper OM, Bastidas N, Kleinman ME, et al. Progenitor cell trafficking is regulated by hypoxic gradients through HIF-1 induction of SDF-1. *Nat Med* 2004;10:858-64.
 15. Isner JM, Asahara T. Angiogenesis and vasculogenesis as therapeutic strategies for postnatal neovascularization. *J Clin Invest* 1999;103:1231-6.
 16. Park S, Tepper OM, Galiano RD, Capla JM, Baharestani S, Kleinman ME, et al. Selective recruitment of endothelial progenitor cells to ischemic tissues with increased neovascularization. *Plast Reconstr Surg* 2004;113:284-93.
 17. Zan T, Li Q, Dong J, Zheng S, Xie Y, Yu D, et al. Transplanted endothelial

- progenitor cells increase neo-vascularisation of rat pre-fabricated flaps. *J Plast Reconstr Aesthet Surg* 2010 ;63:474-81.
18. Kolonin MG, Simmons PJ. Combinatorial stem cell mobilization. *Nat Biotech* 2009;27:252-3.
 19. Pitchford SC, Furze RC, Jones CP, Wengner AM, Rankin SM. Differential mobilization of subsets of progenitor cells from the bone marrow. *Cell stem cell* 2009;4:62-72.
 20. Brave M, Farrell A, Lin SC, Ocheltree T, Miksinski SP, Lee S, et al. FDA review summary: Mozobil in combination with granulocyte colony-stimulating factor to mobilize hematopoietic stem cells to the peripheral blood for collection and subsequent autologous transplantation. *Oncology* 2010;78:282-8.
 21. M. W. Phaffl. A new mathematical model for relative quantification in real-time RT-PCR. *Nucliec Acids Res* 2001;29:e45
 22. De Filippo RE, Atala A. Stretch and growth: the molecular and physiologic influences of tissue expansion. *Plast Reconstr Surg* 2002;109:2450-62.
 23. Tepper OM, Capla JM, Galiano RD, Ceradini DJ, Callaghan MJ, Kleinman ME, et al. Adult vasculogenesis occurs through in situ recruitment, proliferation, and tubulization of circulating bone marrow-derived cells. *Blood* 2005;105:1068-77.
 24. Asahara T, Kawamoto A, Masuda H. Concise review: Circulating endothelial progenitor cells for vascular medicine. *Stem cells* 2011;29:1650-5.
 25. Takahashi T, Kalka C, Masuda H, Chen D, Silver M, Kearney M, et al. Ischemia- and cytokine-induced mobilization of bone marrow-derived

- endothelial progenitor cells for neovascularization. *Nat Med* 1999;5:434-8.
26. Borgquist O, Ingemansson R, Malmsjö M. Wound edge microvascular blood flow during negative-pressure wound therapy: examining the effects of pressures from–10 to–175 mmHg. *Plast Reconstr Surg* 2010;125:502-9.
 27. Yang M, Li Q, Sheng L, Li H, Weng R, Zan T. Bone marrow–derived mesenchymal stem cells transplantation accelerates tissue expansion by promoting skin regeneration during expansion. *Ann Surg* 2011;253:202-9.
 28. Shrader CD, Rissetar HG, Luo J, Cilento EV, Reilly FD. Acute stretch promotes endothelial cell proliferation in wounded healing mouse skin. *ArchDermatol Res* 2008;300:495-504.
 29. Chenwang D, Shiwei B, Dashan Y, Qiang L, Bin C, Muxin Z, et al. Application of botulinum toxin type A in myocutaneous flap expansion. *Plast Reconstr Surg* 2009;124:1450-7.
 30. Tang Y, Luan J, Zhang X. Accelerating tissue expansion by application of topical papaverine cream. *Plast Reconstr Surg* 2004;114:1166-9.
 31. Vinnik CA, Jacob SW. Dimethylsulfoxide (DMSO) for human single-stage intraoperative tissue expansion and circulatory enhancement. *Aesthetic Plast Surg* 1991;15:327-37.
 32. Copcu E, Sivrioglu N, Sisman N, Aktas A, Oztan Y. Enhancement of tissue expansion by calcium channel blocker: a preliminary study. *World J Surg Oncol* 2003;1:1-9.
 33. Zhu X, Hall D, Ridenour G, Boo S, Jennings T, Hochberg J, et al. A mouse

model for studying rapid intraoperative methods of skin closure and wound healing. *Med Sci Monit* 2003;9:109-15.

34. De Falco E, Porcelli D, Torella AR, Straino S, Iachininoto MG, Orlandi A, et al. SDF-1 involvement in endothelial phenotype and ischemia-induced recruitment of bone marrow progenitor cells. *Blood* 2004;104:3472-82.
35. Jujo K. CXCR4 blockade augments bone marrow progenitor cell recruitment to the neovasculature and reduces mortality after myocardial infarction. *Proc Natl Acad Sci USA* 2010;107:11008-13.
36. Erba P, Miele LF, Adini A, Ackermann M, Lamarche JM, Orgill BD, et al. A morphometric study of mechanotransductively induced dermal neovascularization. *Plast Reconstr Surg* 2011;128:288e-99e.
37. Pompilio G, Capogrossi MC, Pesce M, Almanni F, DiCampi C, Achilli F, et al. Endothelial progenitor cells and cardio-vascular homeostasis: clinical implications. *Int J Cardiol* 2009; 131.2: 156-167.
38. Gnechi M, Zhang Z, Ni A, Dzau VJ. Paracrine mechanisms in adult stem cell signaling and therapy. *Circ Res* 2008;103.11: 1204-19.
39. Namba T, Koike H, Murakami K, Aoki M, Makino H, Hashiya N, et al. Angiogenesis induced by endothelial nitric oxide synthase gene through vascular endothelial growth factor expression in a rat hindlimb ischemia model. *Circulation* 2003; 108.18: 2250-57.
40. Amano K, Matsubara H, Iba O, Okigaki M, Fujiyama S, Imada T, et al. Enhancement of ischemia-induced angiogenesis by eNOS overexpression.

Hypertension 2003;41:156–62.

ABSTRACT(IN KOREAN)

확장된 허혈 뇌졸중에서 AMD-3100이 뇌졸중 생존에 미치는 영향

<지도교수 탁관철>

연세대학교 대학원 의학과

정 희 선

넓은 뇌졸중을 얻기 위한 뇌졸중의 확장은 허혈 상태가 지속되면 VEGF의 발현 증가하여 신생혈관생성이 증대되고 이로 인해 뇌졸중의 생존력이 증가한다. 허혈 조직이 있을 시 골수유래 혈관내피 전구세포는 골수로부터 이동, 증식, 분화하여 말초혈액으로 이동한 후 새로운 혈관을 생성에 기여한다. 허혈 상태 또는 VEGF전처치시 CXCR4 억제제인 AMD-3100(plerixafor, Mozobil®)를 투여하면 골수내의 SDF-1과 조혈간세포(hematopoietic stem cell)의 CXCR4간의 결합이 억제되어 조혈간 세포는 말초 혈액내로 이동 및 혈관내피세포전구체로의 분화, 증식이 촉진된다.

본 연구에서는 새로운 조직확장 허혈뇌졸중 동물 모델을 고안하고, 지속적인 허혈에 의한 허혈상태에서 골수유래 혈관내피 전구세포의 이동을 확인하고 이에 AMD-3100의 뇌졸중 생존에서의 역할을 확인하고자 한다.

본 실험은 뇌졸중의 확장 여부와 AMD-3100 투여 여부에 따라 총 40마리의 웅성 백서를 4개의 실험군(n=10)으로 분류하였다(I군(비확장, 비투여), II군(확장, 비투여), III군(비확장, 투여), IV군(확장, 투여). AMD-3100은 수술 후 30분, 24시간, 48시간, 각기 1회씩 도합 3회 뇌졸중 주사를 시행하였다. AMD-3100에 의한 골수유래혈관내피전구세포의 말초혈관으로의 이동은 술

후 1일, 2일 백서의 경골에서 추출한 골수에서 활성 MMP-9의 Zymography에서의 발현 여부와 말초 혈액에서 FACS를 이용하여 골수유래혈관내피전구세포(CD34+ VEGFR2+), VEGFR2, CD133에 양성인 세포의 분획을 조사하였다. 피판의 생존 여부, 신생혈관생성능(CD31) 및 허혈 조직의 성장인자 환경(VEGF, SDF-1, HIF-1 α , NOS3, VEGFR)은 피판의 생존면적 측정, 조직 염색, 레이저미세혈류측정, 단백질 정량 분석(Western blot) 및 정량적 실시간 중합효소연쇄반응(real time quantitative RT-PCR)으로 확인하였다.

골수 내 활성 MMP-9은 AMD-3100 투여한 군(3군, 4군)에서 통계적으로 유의하게 증가하였다($p < 0.05$). AMD-3100투여시비확장 피판 보다 확장 피판의 말초혈액에서 통계적으로 유의하게 골수유래혈관내피세포(EPC, CD34+ VEGFR2+)의 분획이 증가하였으며 확장피판에서는 VEGFR2+ 세포 분획이 증가하였다($p < 0.05$). 예비 실험에서 술 후 7일경 AMD-3100을 투여한 경우 피판 생존율이 증가하였으나, 실리콘을 삽입하는 경우 피판의 생존율이 감소하였다($p < 0.05$). 본 실험에서 술 후 7일째, 피판 생존 면적율과 근위부의 혈류량은 AMD-3100 투여 및 확장 여부와 관련하여 차이가 없었다($p > 0.05$), AMD 3100의 투여 시 혈관의 면적과 개수는 통계학적으로 유의하게 증가하였다($p < 0.05$). VEGF의 발현양은 확장과 AMD-3100이 있었던 경우 모두 통계적으로 유의하게 증가하였으며 SDF-1의 발현은 AMD-3100을 투여한 비확장 피판에서만 통계적으로 유의하게 증가하였다. NOS3와 HIF-1 α 의 발현양은 AMD-3100의 투여와 확장여부와 관계없이 군간에 통계적으로 유의하게 차이를 나타내지 않았다($p > 0.05$).

AMD-3100은 확장 또는 비확장 피판에서 골수로부터 말초혈관으로 골수유래혈관 내피세포를 이동, 분화, 증식을 촉진시켜 피판의 신생혈관을 촉진시켰다. 그러나, 확장기에 의한 피판과 수혜부의 신생혈관의 차단으로 피판의 생존율에 미치는 영향은 없었다.

핵심되는말 : 혈관내피 전구세포, 조혈간세포, 조직확장, 허혈 피판, AMD-3100, CXCR4 억제제